Photoemission study of Ni borocarbides: Superconducting YNi_2B_2C and nonsuperconducting $LaNi_2B_2C$

K. Kobayashi, T. Mizokawa, K. Mamiya, A. Sekiyama, and A. Fujimori
Department of Physics, University of Tokyo, Bunkyo-ku, Tokyo 113, Japan

H. Takagi
Institute for Solid State Physics, University of Tokyo, Roppongi, Tokyo 106, Japan

H. Eisaki and S. Uchida
Department of Applied Physics, University of Tokyo, Bunkyo-ku, Tokyo 113, Japan

R. J. Cava, J. J. Krajewski, and W. F. Peck, Jr.
AT&T Bell Laboratories, Murray Hill, New Jersey 07974

(Received 30 October 1995; revised manuscript received 6 February 1996)

We have studied the electronic structure of Ni borocarbides by means of photoemission and inverse-photoemission spectroscopy. The core-level and valence-band spectra of superconducting YNi_2B_2C and nonsuperconducting $LaNi_2B_2C$ are presented and are compared with band-structure calculations. The core-level spectra well reflect their highly covalent bonding character. The Ni core-level spectra show weak but distinct satellites due to two-hole bound states, indicating significant electron correlation in both compounds. Although the gross electronic structure of both compounds is in agreement with the band-structure calculations except for the two-hole bound-state satellites, spectra near the Fermi level (E_F) are quite different from those predicted by the calculations. That is, high-resolution photoemission spectra do not show a peak at E_F in YNi_2B_2C and that at $\sim$0.1 eV below E_F in $LaNi_2B_2C$, which have been predicted by the calculations, indicating that electron correlation and/or electron-phonon interaction may play a significant role in the low-energy excitations in the Ni borocarbides. A similar behavior in the spectra of *A*15-type superconductors is also pointed out. [S0163-1829(96)02526-X]

I. INTRODUCTION

The recent discovery[1–3] of a new type of superconductor LNi_2B_2C (L = Y, Lu, Ho, Tm, Er, etc.) has invoked renewed interest in intermetallic superconductors. They have rather high critical temperatures (T_c = 16.6 K for L = Lu, T_c = 15.6 K for L = Y) although a late transition element Ni is contained. These borocarbides belong to a new class of superconductors which also includes Pd and Pt compounds. These intermetallic compounds fall into the same region in the γ-T_c plot[4] (γ is the electronic specific heat coefficient) as the *A*15-type compounds and the Chevrel-phase compounds, where both γ and T_c are relatively high. Indeed, competition between superconductivity and magnetism[5] in $HoNi_2B_2C$, for example, is reminiscent of that in $HoMo_6S_8$, one of the reentrant superconductors.[6] Also, the T_c and the estimated thermodynamic critical field H_c of LNi_2B_2C are comparable to those of *A*15-type compounds.[4]

According to band-structure calculations using the local-density approximation (LDA),[7] YNi_2B_2C and $LuNi_2B_2C$ have a high density of states (DOS) at the Fermi level (E_F), which is also the case in the cuprates,[8] *A*15-type compounds,[9] Chevrel-phase compounds,[6] and doped fullerenes,[10] although these compounds have quite different crystal and electronic structures. In the borocarbides, although the Ni 3*d* orbital component has a dominant contribution at E_F, the atomic orbitals of all the other elements also have significant partial DOS at E_F as pointed out in Ref. 11. The borocarbides consist of alternating LC and Ni_2B_2 layers, implying two dimensionality (2D) while the band-structure calculations show 3D rather than 2D character. The high Ni 3*d* partial density of states at E_F suggests that electron correlation may be significant. In fact, a ^{11}B NMR study[12] indicates that antiferromagnetic spin fluctuations appear in the normal state of $LuNi_2B_2C$, and further, the electrical resistivity is proportional to T^2 at low temperatures.[13]

Photoemission spectroscopy is one of the most suitable methods for investigating electronic states in solids. For YNi_2B_2C, we have observed[14] a two-hole bound-state satellite of Ni 3*d* origin at a binding energy (E_B) of $\sim$8 eV using the resonance photoemission technique. The results suggest that electron correlation is significant in the Ni 3*d* band and the on-site *d*-*d* Coulomb interaction energy is as large as $\sim$5 eV. We have also observed that a DOS peak at E_F which is predicted by the band-structure calculations is suppressed and the lost spectral weight is transferred away from E_F. Golden *et al.*[15] have also reported the same Ni satellite in the photoemission spectra. Pellegrin *et al.*[16] have measured Ni 2*p* and B 1*s* core level x-ray absorption (XAS) spectra and found a similarity between the two XAS spectra, which they attributed to strong Ni-3*d*–B-2*p* hybridization.

In what follows, we report on a comparative study of the electronic structures of the superconductor YNi_2B_2C and the nonsuperconductor $LaNi_2B_2C$. Since La is nonmagnetic, it

 © 1996 The American Physical Society

is not trivial why $LaNi_2B_2C$ shows no superconductivity. The band-structure calculations[18] suggest that the change in the coordination geometry of the NiB_4 tetrahedra induced by the change of L from Y to La has a great influence on the *s-p* band of B near E_F. As a result, $LaNi_2B_2C$ has a smaller DOS at E_F than YNi_2B_2C. This sizable effect accompanied by the coupling between the electronic state at E_F and the boron A_{1g} phonons is proposed to be essential in the appearance of superconductivity.[18] In this respect, comparative photoemission and inverse-photoemission spectroscopy studies of both compounds are of great interest.

First, we shall report core-level spectra, which tells us their bonding characters. In addition, we have observed satellites derived from two-hole bound states in the Ni core-level spectra, suggesting that electron correlation is significant in both compounds. Second, we shall report the spectra of occupied and unoccupied states around E_F and make a quantitative comparison of them with the band-structure calculations. One would expect different spectra near E_F for the two compounds, according to the above suggestion. However, we have observed that there is little, if any, difference in the spectra of the occupied states near E_F. Moreover, the predicted DOS peak at E_F was not observed in the spectra of YNi_2B_2C even with higher resolution than in the previous work. This may indicate that the electronic structure is significantly modified by the effects which are not included in the band-structure calculations such as electron-electron correlation and/or electron-phonon interaction.

II. EXPERIMENT

Polycrystalline samples of YNi_2B_2C and $LaNi_2B_2C$ were prepared by arc melting and subsequent annealing. Details of the sample preparation are given in Ref. 2. X-ray photoemission spectroscopy (XPS) measurements were performed using the Mg $K\alpha$ line ($h\nu = 1253.6$ eV) and photoelectrons were collected using a double-pass cylindrical-mirror analyzer. Ultraviolet photoemission spectroscopy (UPS) measurements using the He I and He II resonance lines ($h\nu = 21.2$ eV and 40.8 eV, respectively) were made using a hemispherical analyzer. We also measured inverse-photoemission or bremsstrahlung-isochromat spectroscopy (BIS) spectra by detecting photons of $h\nu = 1486.6$ eV using a quartz monochromator. Calibration and estimation of the instrumental resolution were done using Au evaporated on the surface of the samples after each measurement. These were performed for XPS by defining Au $4f_{7/2} = 84.0$ eV, and for BIS and UPS by measuring the Fermi edge. The total resolution was ~ 1 eV, ~ 35 meV, ~ 80 meV, and ~ 0.7 eV for XPS, He I UPS, He II UPS, and BIS, respectively. XPS and BIS measurements were made at liquid-nitrogen temperature and UPS measurements at ~ 25 K. We also measured the temperature dependence of the He I spectra for YNi_2B_2C between 25 K and 200 K. The samples were scraped with a diamond file and measured under a pressure of $1–4 \times 10^{-10}$ Torr. Scraping was repeated until the O 1*s* XPS signal, which indicates surface contamination, disappeared. As the surface stayed clean for 1–2 h after scraping, all the measurements were undertaken for surfaces scraped repeatedly during this interval.

III. RESULTS AND DISCUSSIONS

A. Core levels

YNi_2B_2C and $LaNi_2B_2C$ both have Ni, B, and C in common. Therefore it is meaningful to compare the B 1*s*, C 1*s*, and Ni 2*p* core-level spectra for the two compounds. The B 1*s* peak position was 188.1 eV and 188.0 eV for YNi_2B_2C and $LaNi_2B_2C$, respectively. These values are similar to those (186–188 eV) reported on binary transition-metal borides such as FeB and CoB by Mavel *et al.*[19,20] This indicates that in LNi_2B_2C the character of bonding between Ni and B is similar to the metal-boron bonding in the simple boride. The same holds for the C 1*s* peak position, which was 282.7 eV and 282.5 eV for YNi_2B_2C and $LaNi_2B_2C$, respectively. These values are in the same range as the C 1*s* peak positions (282 eV) in MC (M = Ti, Zr, and Hf),[20,21] considering that it can vary between 280 eV and 293 eV from compound to compound.[20] The similarity suggests that electrons are transferred from metal (L) to carbon atoms in the nickel borocarbides as in the binary metal carbides. Figure 1 shows the Ni 2*p* core-level spectra of both borocarbides. In $LaNi_2B_2C$, the Ni $2p_{3/2}$ and La $3d_{3/2}$ peaks are at the same position and therefore the spectra of both compounds have been normalized at the Ni $2p_{1/2}$ peak, for which the positions are 870.7 eV and 870.5 eV for YNi_2B_2C and $LaNi_2B_2C$, respectively, while in Ni metal the peak is at 869.7 eV.[20] As Pellegrin *et al.* have remarked,[16] these chemical shifts are supposed to result from charge transfer from the metal atoms (Ni and L) to its nonmetal B and C neighbors, which is again consistent with the above suggestion based on the comparison with the binary metal borides and carbides. The shape of the La $3d_{5/2}$ peak in $LaNi_2B_2C$ is similar to that in La metal rather than ionic compounds like La_2O_3.[22] That is, the well-screened feature at ~ 833 eV is much weaker than the poorly-screened peak at ~ 836.5 eV, reflecting the highly covalent La-C bonding character.

Thus in going from $LaNi_2B_2C$ to YNi_2B_2C, the core levels are shifted towards higher binding energy by 0.1–0.2 eV. Since the crystal structure and the number of conduction electrons are almost the same for both, the core-level shifts may well reflect small differences in bond lengths or bond angles between constituent atoms. In fact, the Ni-Ni bond lengths are 2.50 Å (Ref. 17) and 2.68 Å (Ref. 18) for YNi_2B_2C and $LaNi_2B_2C$, respectively. The shorter bond length tends to increase the width of the Ni 3*d* valence band, which will raise the Fermi level since the E_F is located near the top of the Ni 3*d*-derived valence band. This in turn lowers the core-level positions relative to E_F. This explains the higher binding energies of the core levels in YNi_2B_2C than in $LaNi_2B_2C$.

A remarkable feature in the Ni 2*p* spectra is the existence of a satellite in both compounds, which is around 861 eV for Ni $2p_{3/2}$. Such a satellite is well known in Ni metal and Ni intermetallic compounds[23,24] and is assigned to a ''two-hole bound state'' in the core-hole final state, resulting from significant Coulomb interaction between the core hole and the Ni 3*d* hole. On the other hand, resonance photoemission from the valence band of YNi_2B_2C has revealed a satellite around the binding energy of 8–9 eV.[14,15] The satellite posi-

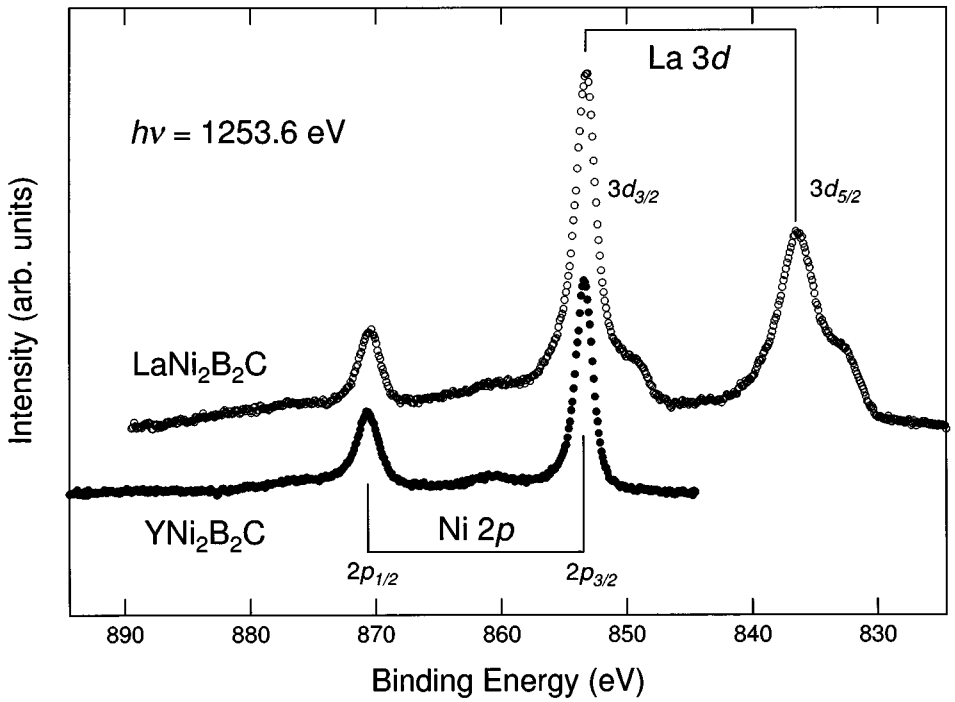

FIG. 1. Ni 2*p* core-level photoemission spectra of YNi_2B_2C and $LaNi_2B_2C$. They are normalized at the Ni $2p_{1/2}$ peak.

tion is ~7 eV away from the main peak for the Ni $2p_{3/2}$ core level and ~7 eV from the main Ni 3*d* peak for the valence band.

B. Valence-band photoemission spectra

Figure 2 shows the valence-band XPS spectra of YNi_2B_2C and $LaNi_2B_2C$ measured at liquid-nitrogen temperature and the He I and He II UPS spectra measured at ~25 K. These spectra have been normalized to the peak height. To what extent the contribution of each constituent element appears in the spectra depends on the cross sections as listed in Table I.[26]

The XPS spectra of both compounds are shown at the bottom of Fig. 2. The satellite structure due to the two-hole bound state at binding energy E_B~8 eV is weak. (The satellite in the XPS spectra can be identified as an excess intensity at E_B~8 eV compared to the band structure calculation; see Fig. 5 and Sec. III D.) Judging from Table I, the XPS spectra reflect mainly Ni 3*d* character. The He II UPS spectra are shown in the middle panel of Fig. 2. Considering the photoionization cross sections, the He II spectra reflect more B and C 2*sp* character than the XPS spectra. The intensity of the He II spectra at $E_B>4$ eV is stronger than that of the XPS spectra, which indicates the existence of a broad B and C 2*sp* band at $E_B>4$ eV. The He I spectra are also shown at the top of Fig. 2. Much more B and C 2*sp* and much less Ni 3*d* character should appear in the He I spectra than in the He II spectra according to Table I, and therefore the feature around 4–5 eV is certainly of B and C 2*sp* character. These results agree well with those of B 1*s* soft x-ray emission spectroscopy (SXES),[25] which show a large peak around 4–5 eV for both compounds. However, there are additional intense features around 6–7 eV in our He I spectra. They may be due to surface contamination in grain boundaries of the polycrystalline samples, because the bulk-sensitive SXES spectra shows no such feature there.

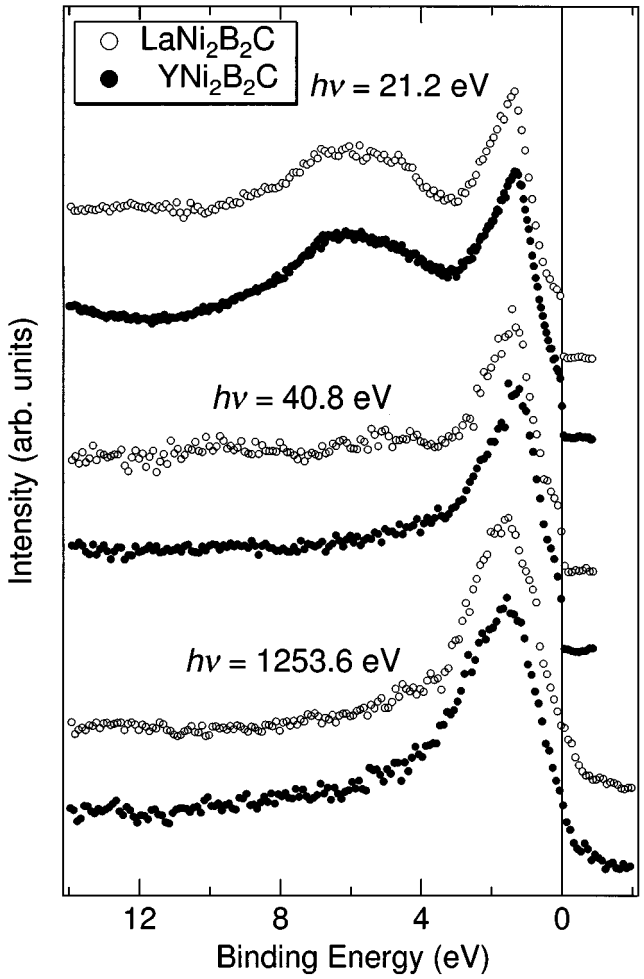

FIG. 2. Valence-band photoemission spectra of YNi_2B_2C and $LaNi_2B_2C$.

TABLE I. Cross sections per electron of the atomic orbitals relative to Ni 3*d* (Ref. 26). ''B 2*sp*'' gives an average over B 2*s* and B 2*p* and so on. The B and C 2*sp* cross sections have been multiplied by an empirical factor of 3 (Ref. 27).

Photon energy (eV)	B 2*sp*	C 2*sp*	Y 4*d*	La 5*d*
21.2	8.4	11.1	9.6	8.2
40.8	1.4	2.2	0.49	0.50
1253.6	0.29	0.60	0.58	0.88
1486.6	0.28	0.67	0.61	1.0

In the He I spectra of the two compounds, the main peak due to Ni 3*d* is at the same position and the intensity just below E_F is essentially the same, which is also the case for the He II spectra. The intensity just at E_F relative to the intensity of the peak at $\sim$1.4 eV increases in going from $h\nu$=21.2 eV to $h\nu$=40.8 eV. Because the relative cross sections of Ni 3*d* to B and C 2*sp* increase when going from $h\nu$=21.2 eV to $h\nu$=40.8 eV, we may say that the contribution of Ni 3*d* is large at E_F in both compounds. The spectra of YNi_2B_2C and $LaNi_2B_2C$ closely resemble each other at each photon energy, while they differ in that the YNi_2B_2C spectra show a shoulder structure around 2 eV,[25] but that no such structure can be seen in the $LaNi_2B_2C$ spectra. The presence of the shoulder structure is consistent with the band-structure calculations as discussed below.

In addition, we have measured spectra of YNi_2B_2C near E_F in detail with changing temperature from 25 K to 200 K as shown in Fig. 3. As the temperature increases, the slope of the spectrum at the Fermi level decreases systematically, which can be explained by the temperature dependence of the Fermi-Dirac distribution function. We find no evidence for the peak at E_F predicted by the band-structure calculations even with 3 times higher resolution than in the previous work.[14]

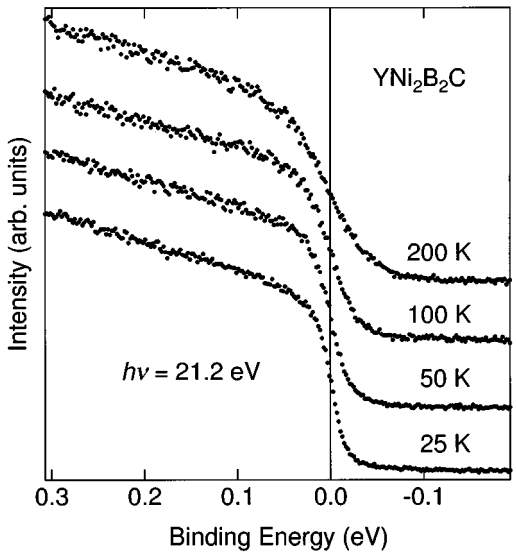

FIG. 3. Temperature dependence of the UPS spectra of YNi_2B_2C near E_F.

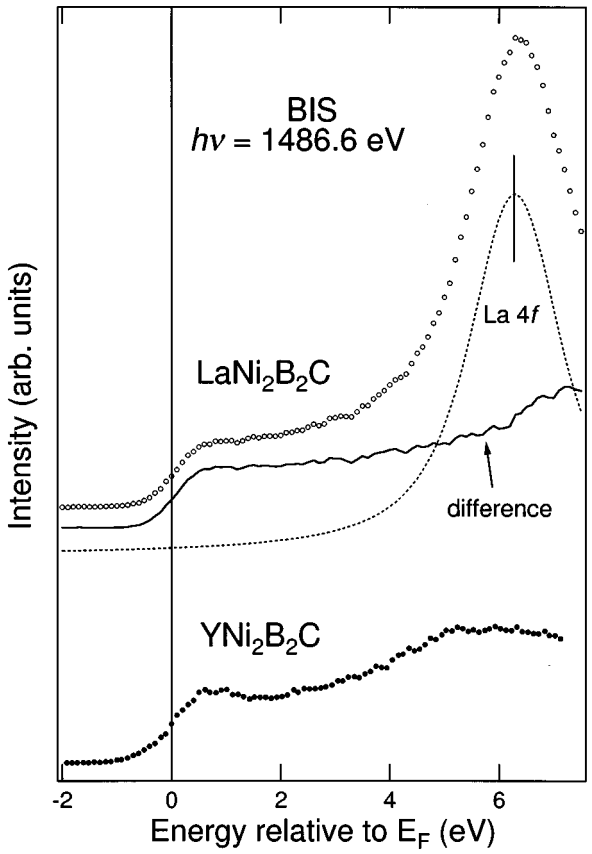

FIG. 4. BIS spectra of YNi_2B_2C and $LaNi_2B_2C$. The dashed line is a fitted line shape for the La 4*f* empty states.

C. BIS spectra

Figure 4 shows BIS spectra of YNi_2B_2C and $LaNi_2B_2C$. The intense peak at $\sim$6 eV in the $LaNi_2B_2C$ spectrum is assigned to the La 4*f* empty states while the band-structure calculations[18] have predicted the 4*f* states to be around 3 eV above E_F. In order to subtract the influence of the La 4*f* peak from the spectrum, we have performed a line-shape fitting of this peak under the assumption that the peak is given by a convolution of Lorentzian and Gaussian functions, corresponding to the lifetime broadening and the instrumental resolution, respectively. The result is shown in Fig. 4 by a dashed line. The solid line is the difference between the spectrum and the fitted curve. We thus find that the La 4*f* peak has little influence on the spectrum near the Fermi level, and therefore we can compare the BIS spectrum of $LaNi_2B_2C$ with the band-structure calculations as described below.

D. Comparison with the band-structure calculations

We have performed detailed comparison between the photoemission spectra and theoretical spectra derived from the band-structure calculations.[7,18] The result is shown in Figs. 5 and 6. To obtain the theoretical photoemission spectra, the partial DOS of each atomic orbital component, namely, the La 5*d* or Y 4*d*, Ni 3*d*, B 2*sp*, and C 2*sp* partial DOS, have been added after having multiplied by the corresponding photoionization cross sections at each photon energy (Table I). Then this weighted DOS has been broadened

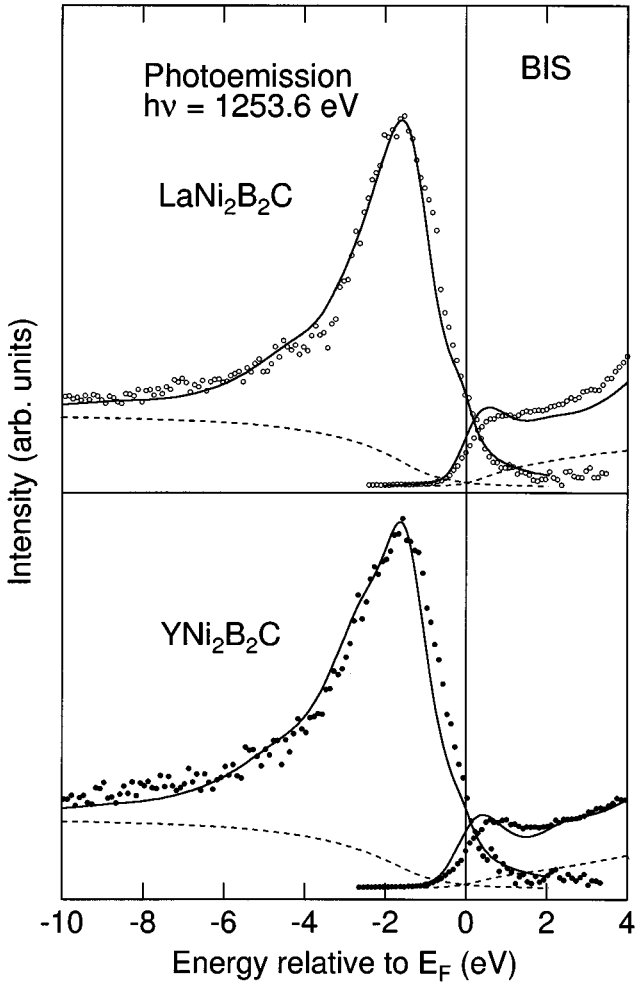

FIG. 5. Comparison of the XPS and BIS spectra (dots) with the theoretical spectra derived from the band-structure calculations (Refs. 7,18) (solid curves). The dashed lines show the integral background.

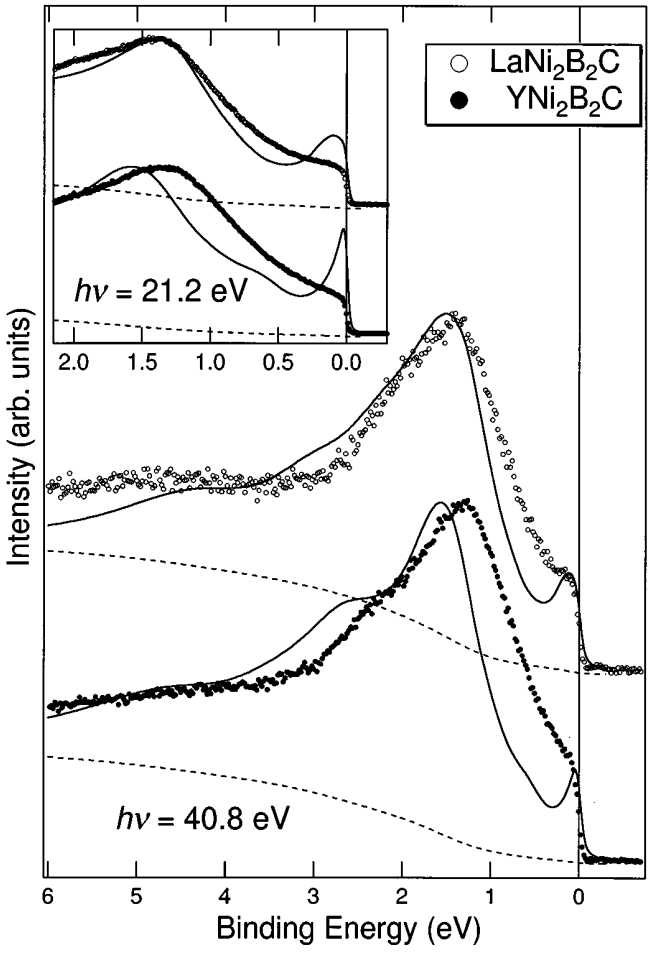

FIG. 6. Comparison of the He I and He II UPS spectra (dots) with the theoretical spectra derived from the band-structure calculations (Refs. 7,18) (solid curves). The dashed lines show the integral background.

by convoluting with a Gaussian and a Lorentzian which represent the instrumental resolution and the lifetime broadening, respectively. We postulate that the lifetime width is linear in energy E measured from E_F, i.e., the full width at half maximum (FWHM) $w=\alpha|E-E_F|$, where the constant α is a parameter which is determined so as to well simulate the measured spectra. For both compounds we have taken $\alpha=0.30$ for the photoemission spectra. In simulating the spectra, we have also added an integral background due to secondary electron emission as shown by dashed lines in Figs. 5 and 6. Normalization between the experimental and theoretical spectra has been done at the peak height.

To obtain the theoretical BIS spectra, we have proceeded in the same way as for the photoemission spectra, except that we have taken $\alpha=0.20$. The BIS spectra reflect the Ni 3*d* and Y 4*d* or La 5*d* components of the empty states because the B and C 2*sp* components have small cross sections at $h\nu=1486.6$ eV and small DOS above E_F.[7,18] As for the BIS spectrum of $LaNi_2B_2C$, however, the calculated DOS cannot be directly compared with the experimental data because of the large discrepancy in the position of the La 4*f* empty state. Therefore we compare the Ni 3*d* partial DOS plus the La 4*f* peak which has been fitted to the Lorentzian-Gaussian as described above and shifted to ~ 6 eV above E_F (Sec. III C) as shown in Fig. 5.[28] The normalization between the photoemission and BIS spectra in Fig. 5 has been done so that the measured spectra nearly match the calculated DOS.

Comparison between the experimental photoemission spectra and the theoretical ones supports our discussion in Sec. III B. The feature due to the broad B and C 2*sp* bands around 4–5 eV can be seen in the theoretical spectra at $h\nu=$ 40.8 eV and 1253.6 eV, which agree quite well with the experimental spectra even in the quantitative sense, as in the case of the SXES result.[25] The shoulder at ~ 2 eV in the measured spectra of YNi_2B_2C is also seen in the calculated Ni 3*d* partial DOS,[7] although the position is somewhat shifted. Concerning this point, the band-structure calculations well reproduce the difference between YNi_2B_2C and $LaNi_2B_2C$.

However, some discrepancies exist between theory and experiment. First of all, the XPS spectra (Fig. 5) show additional intensity at $E_B\sim 8$ eV compared to the band DOS, which we attribute to a two-hole bound state satellite in analogy with the Ni core-level spectra. Second, Fig. 6 shows that the DOS peak just at E_F of YNi_2B_2C is not observed. As for $LaNi_2B_2C$, the DOS peak exists about 0.1 eV below E_F in

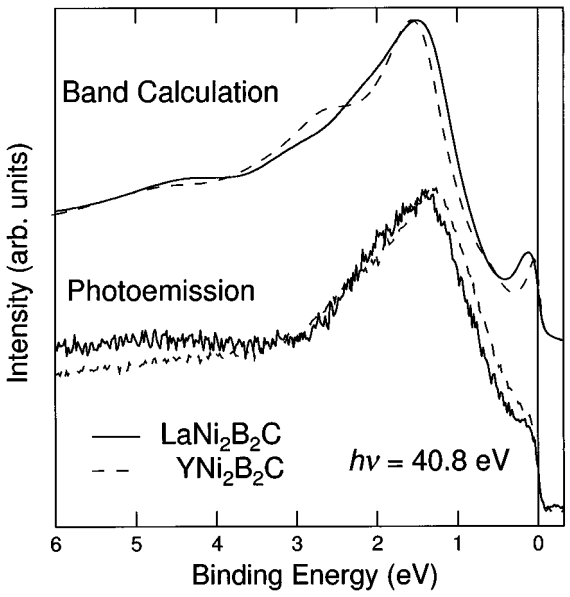

FIG. 7. Comparison of the He II UPS spectra between YNi_2B_2C (solid curve) and $LaNi_2B_2C$ (dashed curve). The theoretical spectra derived from the band-structure calculations (Refs. 7,18) are shown in the upper panel and the experimental spectra in the lower panel.

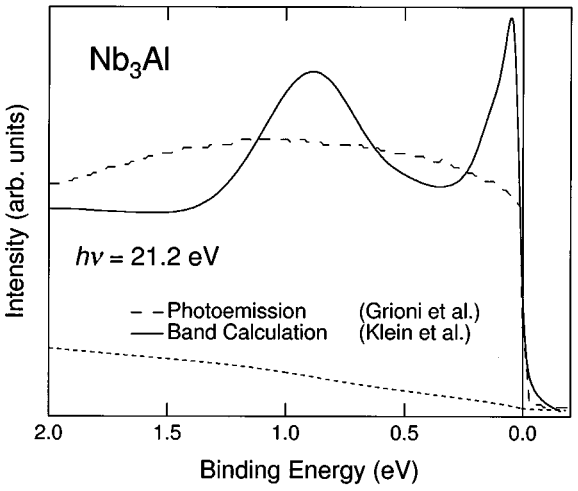

FIG. 8. Comparison between the experimental spectra (Ref. 30) and the theoretical spectra derived from the band-structure calculations (Ref. 9) of a *A*15-type compound Nb_3Al.

the theoretical spectrum, but there is no sign of the corresponding peak structure in the measured spectra. Another weak structure around 0.7 eV below E_F seen in the theoretical curve of YNi_2B_2C is also suppressed. Third, the Ni 3*d* peak position $E_B \sim 1.4$ eV of YNi_2B_2C is not in good agreement with the band-structure calculations. At each photon energy, one can see that the peak structure itself is shifted by ~ 0.2 eV toward the Fermi level compared to the band-structure calculation. As for the counterpart in $LaNi_2B_2C$, there is better agreement between experiment and theory. As a result, the shift of the Ni 3*d* peak in going from YNi_2B_2C to $LaNi_2B_2C$ is opposite between the theoretical spectra and the experimental ones as shown in Fig. 7, where the spectra of the two compounds are plotted together.

One can see in Fig. 6 that the theoretical intensity at the Fermi level for $h\nu = 21.2$ eV is twice as large as the experimental intensity in both compounds, while that for $h\nu = 40.8$ eV is of the same level although no peak structure is observed at either photon energy. This may imply that the B and C 2*sp* weights at E_F are overestimated in the band-structure calculations, since the relative cross sections of B and C 2*sp* to Ni 3*d* increase with decreasing photon energy (Table I).

The theoretical BIS spectra shown in Fig. 5 also discriminate between YNi_2B_2C and $LaNi_2B_2C$. In YNi_2B_2C, the calculated BIS spectrum has a higher intensity at E_F than in $LaNi_2B_2C$, reflecting the sharp DOS peak at E_F in YNi_2B_2C, but the measured spectra of both compounds show ordinary Fermi edges. Pellegrin *et al.*[16] have measured the Ni L_3-edge XAS spectra of the Ni borocarbides and found good agreement with the band-structure calculations. However, if we take into account the uncertainty in the Fermi level position in XAS measurements, their XAS results are consistent with our BIS spectrum of YNi_2B_2C.

The above discrepancies between theory and experiment near E_F may occur due to effects which are not included in the band-structure calculations, namely, electron correlation and/or electron-phonon interaction. These interactions will generally result in a mass enhancement and spectral weight transfer away from E_F on the low-energy scale. In YNi_2B_2C, the electronic specific heat coefficient γ is ~ 1.8 times enhanced to be 18.2 mJ/mol K^2 (Ref. 29) compared to that given by the band-structure calculations. Electron-phonon interaction may be significant because of the existence of the high-frequency boron A_{1g} phonon, whose frequency has been calculated to be 106 meV.[11] We stress here that the suppression of the DOS peak at E_F does not mean a disappearance of the states at E_F, but that the lost spectral weight is transferred to higher energies. As for the opposite shifts of the Ni 3*d* peak in going from the La to the Y compounds between the theoretical spectra and the experimental ones in Fig. 7, electron correlation probably influences the Ni 3*d* spectral weight distribution. This does not preclude the possibility that the difference in the B, C 2*sp*-derived bands as predicted by the band-structure calculations[18] is responsible for the different superconducting properties. Indeed, the SXES study has revealed differences in the B 1*s* spectra between the Y and La compounds[25] as predicted by the band-structure calculations.[18]

It is instructive to compare the present results with the results for similar intermetallic superconductors. Figure 8 shows a high-resolution photoemission spectrum of Nb_3Al, a member of the *A*15-type compounds, by Grioni *et al.*[30] It shows superconductivity below 18.6 K, and has a large DOS at E_F according to the band-structure calculation by Klein *et al.*[9] In addition, the relation between the electronic specific heat coefficient and the critical temperature (γ-T_c plot[4]) shows that the *A*15-type compounds are located close to the Ni borocarbides. We obtain the theoretical spectrum of Nb_3Al from the band-structure calculation as described above. The peak just at E_F in the calculated DOS has been suppressed and the fine structures near E_F have been smeared out. This is apparently inconsistent with the electron-energy-loss study of Nb_3Al, where a prominent

peak has been observed at E_F.[31] However, this peak arises from a step in the DOS on the high-energy side and the Fermi cutoff on the low-energy side convoluted with the energy resolution of 0.2 eV and is not directly related to the peak which one would expect to observe with the resolution of a few tens meV. The disappearance of the DOS peak at E_F was previously suggested by Ho *et al.*[32] in the context of lifetime broadening due to strong electron-phonon scattering. On the other hand, it has to be remarked that the angle-resolved photoemission spectra of another *A*15-type compound V_3Si show dispersing features near E_F, which qualitatively agrees with band-structure calculations.[33] Although electron correlation and/or electron-phonon interaction is likely to be responsible for the unusual spectral behavior near E_F, their mechanisms remain to be examined.

IV. CONCLUSION

We have measured photoemission and inverse-photoemission spectra of superconducting YNi_2B_2C and nonsuperconducting $LaNi_2B_2C$. The core-level spectra well reflect their bonding character. We have observed satellites due to two-hole bound states in the Ni core-level and valence-band spectra. The valence-band spectra of both compounds resemble each other and gross spectral features are in good agreement with the band-structure calculations. The contribution of Ni 3*d* to E_F is found to be large. However, there is no sharp DOS peak at E_F, which is predicted by the band-structure calculations. The discrepancy between the band-structure calculations and experiment near the Fermi level is larger in YNi_2B_2C than in $LaNi_2B_2C$. The discrepancy between experiment and theory may be due to electron correlation and/or electron phonon interaction which is not included in the LDA band-structure calculations. It is pointed out that the predicted DOS peak is also absent in other superconductors like *A*15-type materials. It remains to be clarified how the observed differences in the spectra of YNi_2B_2C and $LaNi_2B_2C$ and their agreement and disagreement with the LDA band-structures are related to the occurrence of superconductivity in YNi_2B_2C.

ACKNOWLEDGMENTS

The results of the band-structure calculations including unpublished results were kindly provided by Dr. L. F. Mattheiss. We are greatly indebted to Professor S. Shin for valuable discussions. The work at the University of Tokyo is supported by a Grant-in-Aid for Scientific Research from the Ministry of Education, Science and Culture of Japan.

[1] R. J. Cava, H. Takagi, B. Batlogg, H. W. Zandergen, J. J. Krajewski, W. F. Peck, Jr., R. B. van Dover, R. J. Felder, T. Siegrist, K. Mizuhashi, J. O. Lee, H. Eisaki, S. A. Carter, and S. Uchida, Nature **367**, 146 (1994).

[2] R. J. Cava, H. Takagi, H. W. Zandergen, J. J. Krajewski, W. F. Peck, Jr., T. Siegrist, B. Batlogg, R. B. van Dover, R. J. Felder, K. Mizuhashi, J. O. Lee, H. Eisaki, S. A. Carter, and S. Uchida, Nature **367**, 252 (1994).

[3] R. Nagarajan, C. Mazumdar, Z. Hossain, S. K. Dhar, K. V. Gopalakrishnan, L. C. Gupta, C. Godart, B. D. Padalia, and R. Vijayaraghavan, Phys. Rev. Lett. **72**, 274 (1994).

[4] H. Takagi, R. J. Cava, H. Eisaki, J. O. Lee, K. Mizuhashi, B. Batlogg, S. Uchida, J. J. Krajewski, and W. F. Peck, Jr., Physica C **228**, 389 (1994).

[5] H. Eisaki, H. Takagi, R. J. Cava, B. Batlogg, J. J. Krajewski, W. F. Peck, Jr., K. Mizuhashi, J. O. Lee, and S. Uchida, Phys. Rev. B **50**, 647 (1994).

[6] *Superconductivity in Ternary Compounds*, edited by Ø. Fischer and M. B. Maple (Springer-Verlag, Berlin, 1982), Vols. I and II.

[7] L. F. Mattheiss, Phys. Rev. B **49**, 13279 (1994); and (unpublished).

[8] A. J. Freeman, J. Yu, and C. L. Fu, Phys. Rev. B **36**, 7111 (1987).

[9] B. M. Klein, L. L. Boyer, D. A. Papaconstantopoulos, and L. F. Mattheiss, Phys. Rev. B **18**, 6411 (1978); W. E. Pickett, K.-M. Ho, and M. L. Cohen, *ibid.* **19**, 1734 (1979).

[10] S. C. Erwin and W. E. Pickett, Science **254**, 842 (1991).

[11] W. E. Pickett and D. J. Singh, Phys. Rev. Lett. **72**, 3702 (1994).

[12] K. Ikushima, J. Kikuchi, H. Yasuoka, R. J. Cava, H. Takagi, J. J. Krajewski, and W. F. Peck, Jr., J. Phys. Soc. Jpn. **63**, 2878 (1994).

[13] H. Takagi, R. J. Cava, H. Eisaki, S. Uchida, J. J. Krajewski, and W. F. Peck, Jr., in *Advances in Superconductivity VII*, edited by K. Yamafuji and T. Morishita (Springer-Verlag, Tokyo, 1995), p. 9.

[14] A. Fujimori, K. Kobayashi, T. Mizokawa, K. Mamiya, A. Sekiyama, H. Eisaki, H. Takagi, S. Uchida, R. J. Cava, J. J. Krajewski, and W. F. Peck, Jr., Phys. Rev. B **50**, 9660 (1994).

[15] M. S. Golden, M. Knuper, M. Kielwein, M. Buchgeister, J. Fink, D. Teehan, W. E. Pikket, and D. J. Singh, Europhys. Lett. **28**, 369 (1994).

[16] E. Pellegrin, G. Meigs, C. T. Chen, R. J. Cava, J. J. Krajewski, and W. F. Peck, Jr., Phys. Rev. B **51**, 16159 (1995).

[17] T. Siegrist, H. W. Zandbergen, R. J. Cava, J. J. Krajewski, and W. F. Peck, Jr., Nature **367**, 254 (1994).

[18] L. F. Mattheiss, T. Siegrist, and R. J. Cava, Solid State Commun. **91**, 587 (1994).

[19] G. Mavel, J. Escard, P. Costa, and J. Castaing, Surf. Sci. **25**, 109 (1973).

[20] *Handbook of X-Ray Photoelectron Spectroscopy*, edited by C. D. Wagner, W. M. Riggs, L. E. Davis, J. F. Moulder, and G. E. Muilenberg (Perkin-Elmer, City, MN, 1978).

[21] L. Ramqvist, K. Hamrin, G. Johansson, A. Fahlman, and C. Nordling, J. Phys. Chem. Solids **30**, 1835 (1969).

[22] S. Hüfner, in *High Energy Spectroscopy, Handbook on the Physics and Chemistry of Rare Earths*, Vol. 10, edited by K. A. Gschneider, Jr., L. Eyring, and S. Hüfner (North-Holland, Amsterdam, 1987).

[23] D. R. Penn, Phys. Rev. Lett. **42**, 921 (1979); L. C. Davis and L. A. Feldkamp, J. Appl. Phys. **50**, 1994 (1979).

[24] S. Hüfner and G. K. Wertheim, Phys. Lett. **51A**, 299 (1975).

[25] S. Shin, A. Agui, M. Watanabe, M. Fujisawa, Y. Tezuka, T. Ishii, K. Kobayashi, A. Fujimori, and H. Takagi, Phys. Rev. B **52**, 15082 (1995).

[26] J.-J. Yeh and I. Lindau, At. Data Nucl. Data Tables **32**, 1 (1985).

[27] G. A. Sawatzky and D. Post, Phys. Rev. B **20**, 1546 (1979).
[28] The La 5*d* partial DOS is not given in Refs. 7 and 18. Although the cross sections of La 5*d* and Ni 3*d* at $h\nu = 1486.6$ eV are comparable, the calculated partial DOS of Ni is at least twice as large as that of La in the energy range between 0 and 1 eV above E_F, which would justify the comparison between the measured spectrum and the Ni partial DOS.
[29] N. H. Hong, H. Michor, M. Vybornov, T. Holubar, P. Hundegger, W. Perthold, G. Hilscher, and P. Rogl, Physica C **227**, 85 (1994); S. A. Carter, B. Batlogg, R. J. Cava, J. J. Krajewski, W. F. Peck, Jr., and H. Takagi, Phys. Rev. B **50**, 4216 (1994).
[30] M. Grioni, D. Malterre, B. Dardel, J.-M. Imer, Y. Baer, J. Muller, J. L. Jorda, and Y. Petroff, Phys. Rev. B **43**, 1216 (1991).
[31] Th. Müller-Heinzerling, J. Fink, and W. Weaver, Phys. Rev. B **32**, 1850 (1985).
[32] K.-M. Ho, M. L. Cohen, and W. E. Pickett, Phys. Rev. Lett. **41**, 815 (1978).
[33] M. Aono, F. J. Himpsel, and D. E. Eastman, Solid State Commun. **39**, 225 (1981).